

PQ data compression algorithm with modified quantizer and adaptive band logic using DTCWT

EKANTHAI AH PRATHIBHA¹, ASHWATHNARAYAN MANJUNATHA¹, CYRIL PRASANNA RAJ²

¹ Sri Krishna Institute of Technology

No 29, Chimney hills Chikkabanavara post, Bangalore-560090, Karnataka, India

² MS Engineering College Navarathna Agrahara

Sadahalli Post, Bengaluru - 562 110, Karnataka, India

e-mail: prathibha.skit/manjuprinci/cyrilyahoo@gmail.com

(Received: 13.08.2017, revised: 12.01.2018)

Abstract: With growing demand for energy, power generated in renewable sources at various locations are distributed throughout the power grid. The power grid known as the smart grid needs to monitor power generation and its smart distribution. Smart meters provide solutions for monitoring power over smart grids. Smart meters need to continuously log data and at every source there is a large amount of data generated that needs to be compressed for both storage and transmission over the smart grid. In this paper, a novel algorithm for PQ data compression is proposed that uses the Dual Tree Complex Wavelet Transform (DTCWT) for sub-band computation and a modified quantizer is designed to reduce sub-band coefficient limits to less than 4 bits. The Run Length Encoding (RLC) and Huffman Coding algorithm encode the data further to achieve compression. The performance metrics such as a peak-signal-to-noise ratio (PSNR) and compression ratio (CR) are used for evaluation and it is found that the modified DTCWT (MDTCWT) improves PSNR by a factor of 3% and the mean squared error (MSE) by a factor of 16% as compared with the DTCWT based PQ compression algorithm.

Key words: complex wavelets, data compression, power quality disturbances, smart grid

1. Introduction

Technological development have led to the use of Information and Communication Technology (ICT) for power generation, distribution and monitoring. The smart grid is one such technology where micro level monitoring of power generation and distribution is effectively managed. With the smart grid technology going to become reality in the next ten years, the market for the smart grid is predicted to be \$ 50 billion [1]. One of the key components of the smart grid technology is a smart meter. The smart meter will be installed to monitor the power flow from the mains to individual entities in both directions. The data from individual entities can contain information

on power consumption, power generated, harmonics, billing etc. Monitoring smart grid operation and smart meters in real time involves large volumes of data. If the smart meter records continuous data from every entity at a 15 minute time interval, there would be 96 million data records for every million meters. The data gathered from the smart meters provides analysis in terms of customer segmentation, behaviour, better management of energy use and allows them to cut their energy consumption costs. One of the critical activities of the smart meter is to monitor power line disturbances such as voltage sag, swell, harmonics and interrupts. Voltage fluctuations can cause productivity losses [2] and hence it is required to be monitored. Real time monitoring of a PQ signal is based on data logging from the smart meter and this data will be measured in Gigabytes [3] [4]. For data logging, monitoring and analytics of larger amounts of data it is required to compress data and transmit data over the power line. In [5], compression of power quality disturbance data based on wavelet transform combined with an adaptive arithmetic encoding scheme is proposed, demonstrating a 7.09% compression ratio (CR) and 1.42×10^{-3} normalized mean-square error (NMSE) compared with a wavelet coefficient threshold of 13.67% CR and 1.88×10^{-3} NMSE for voltage sag. In [6], in order to improve the compression ratio, difference in input samples are taken as input to a compression algorithm based on Huffman coding. In [7], input data is transformed into wavelet sub-bands to obtain multi-resolutions, from which the PQ disturbances are selected and noise is eliminated in order to achieve higher compressions. In [8], an adaptive quantization technique is proposed to select significant data from the PQ signals after Park's transform. The quantizers are designed based on predictive logic so that an inverse process is carried out without loss during a reconstruction process. The process of transformation from the time to wavelet domain has advantages helping to select info from sub-bands based on significant information. In [10], the techniques are based on wavelet theory and multi-resolution analysis. Any cases of distortion are decomposed into three resolution levels. By using a data compression technique, power quality disturbances are reconstructed. In [11] the author presents the method that combines the compactly supported orthogonal wavelet db4 with the threshold method of minimax theorem to compress power quality disturbance signals. The MATLAB simulation shows that this method can compress the power quality disturbance data effectively, it can obtain a high compression ratio under the premise of no losing the time-frequency local characters. In [12] an advanced metering system (AMI) is a new advanced metering system for a two-way measurement and interaction operation in the smart grid. A compressed sensing (CS) approach based on two-dimensional image compression for power quality analysis is proposed. Since the sampling information of power quality (PQ) has outstanding frequency-domain sparse characteristics, power quality measurement using compressed sensing, a two-dimensional sparse measurement model on voltage, current and power signals was generated. Using these samples, a power signal is recovered in order to effectively detect the operating status of the power quality parameters connecting harmonic, instantaneous power disturbance, etc. The performance of the proposed approach is compared with respect to a compression sampling ratio (CSR), signal-to-noise-ratio (SNR), mean squared error (MSE) as well as energy recovery percentage (ERP). In [13] the compression technique is performed through signal decomposition, threshold of wavelet transform coefficients, and signal reconstruction. Threshold values are determined by weighting the absolute maximum value at each scale. Wavelet transform coefficients whose values are below the threshold are discarded, while those that are above the threshold are kept along with their temporal locations. Therefore, the cost related to storing and transmitting the data is significantly

reduced. In [14] the author presented an attempt to deal with large volume of data made available from various measurement systems, while considering the availability of a referential source in the time domain. Two issues were treated as equally important for the optimization of data storage and features accessibility and the on-line, secure communication with the installed monitoring devices, considering their IP-addressability within a geographical area without appropriate communication infrastructure. In [15], the author proposed the power quality monitoring system that would create huge amounts of data, particularly in time-absorbing and high-rate sampling. This work presents an enhanced method for compressing power quality data based on wavelet transformation. The power quality data, which eliminated fundamental wave is processed with the wavelet transform, and then, the threshold method is used to the wavelet coefficients. Several variety of power quality data were processed by Matlab.

1.1. Discrete Wavelet Transform (DWT)

A wavelet plays an important role in signal processing applications, wavelet transform of an input signal generates multiple sub-bands of low-pass and high-pass wavelet coefficients. The low-pass and high-pass band coefficients provide information on an input signal property. One of the important properties of wavelet coefficients is the de-correlation of low-pass and high-pass frequency information present in the input data. The low-pass coefficients hold the DC levels or intensity levels of the input data and the high-pass data holds the short-duration events in the input signal. Figure 1 presents the level-1 wavelet decomposition using LPF and HPF filters to generate Y_a and Y_d coefficients and Figure 2 presents the reconstruction filters that reconstruct the original signal X from the wavelet coefficients, which is also called the Inverse Discrete Wavelet Transform (IDWT). For perfect reconstruction, the LPF and HPF need to satisfy an orthogonal property. For data compression, multi-level wavelet decomposition is carried out to obtain multi-band frequency components. The most significant sub-bands are the low-pass coefficients and a few high-pass bands. The quantization process retains the information in the low-pass bands and selects information from the high-pass bands. Daubcheies and Haar wavelet filters are primarily used for DWT.

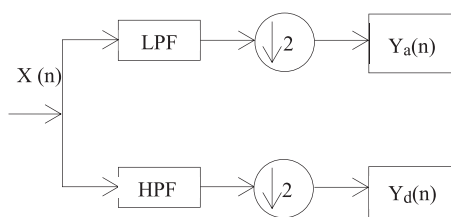


Fig. 1. Basic building block of DWT

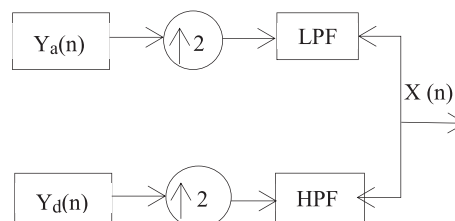


Fig. 2. Basic building block of IDWT

The limitations of the wavelet transform are the shift variance and loss of directional selectivity. The power fluctuations can lead to time delays in PQ signals being monitored and using the DWT will lead to change in PQ signal metrics, as the DWT is the shift variance. The use of the Dual Tree Complex Wavelet Transform (DTCWT) will overcome shift variance limita-

tions, as the DTCWT has real and imaginary filters that generate wavelet coefficients that are shift invariant. The complexity in computation has limited the use of the DTCWT in place of the DWT for data compression. In this paper, a novel algorithm based on the DTCWT is proposed to compress PQ signals and suitable encoding schemes are presented to compress the PQ signals achieving higher compression. Section 2 presents brief introduction to the DTCWT, Section 3 discusses the proposed PQ data compression algorithm based on the DTCWT, Section 4 presents the experimental setup and flow diagram for software implementation of the proposed algorithm. Section 5 presents the results, and the conclusion is presented in Section 6.

2. DTCWT algorithm

DTCWT decomposes an input signal to low-pass and high-pass sub-bands similar to DWT but also generates imaginary sub-bands in addition to real sub-bands. The wavelet filter coefficients for computation of real and imaginary sub-bands are orthogonally shifted and are related by Hilbert transform. With real and imaginary sub-bands time invariant property is achieved and the energy levels of both real and imaginary sub-bands are invariant with redundancy shift in the input signal that is considered for analysis. The DTCWT generates $2N$ sub-bands as compared with the DWT, from these $2N$ sub-bands it is easy to estimate the shift variations in the input signal. The primary challenge in the use of the DTWT for signal processing is the redundancy in data, and it is required to select appropriate sub-bands for data compression. The complex wavelet transform is represented by Equation (1):

$$\psi(t) = \psi_n(t) + j\psi_g(t), \quad (1)$$

where, $\psi_g(t)$ is the Hilbert transform of $\psi_n(t)$.

The input signal $S(z)$ is decomposed into low-frequency part $S_l^1(z)$ and high frequency part $S_h^1(z)$ and can be represented as in Equation (2):

$$S(z) = S_l^1(z) + S_h^1(z), \quad (2)$$

where

$$S_l^1(z) = C^1(z^2)H_0(z^{-1}) \quad \text{and} \quad S_h^1(z) = D^1(z^2)H_1(z^{-1}).$$

The DTCWT algorithm for four-level decomposition is shown in Figure 3. The input signal represented by X , consisting of N samples is decomposed to 10 sub-bands, representing real and imaginary bands of DTCWT outputs, consisting of $N/16$ samples. The transform is twice as expansive, because it generates $2N$ DWT coefficients for an N -point input signal.

The DTCWT algorithm with four levels of decomposition generates ten sub-bands denoted by $\{C_a^4, D_a^4, D_a^3, D_a^2, D_a^1, C_b^4, D_b^4, D_b^3, D_b^2, \text{and } D_b^1\}$. The subscripts 'a' and 'b' denote the real and imaginary trees. C represents the approximation output, D represents the detail output. The subscripts represent the levels. The parameters C_a^4 and C_b^4 obtained at level-4 represent the real and imaginary low-pass coefficients, respectively. The low-pass coefficients contain the lowest band of a PQ signal (pure sine wave) and the high-pass band contains the detail features such as PQ disturbances.

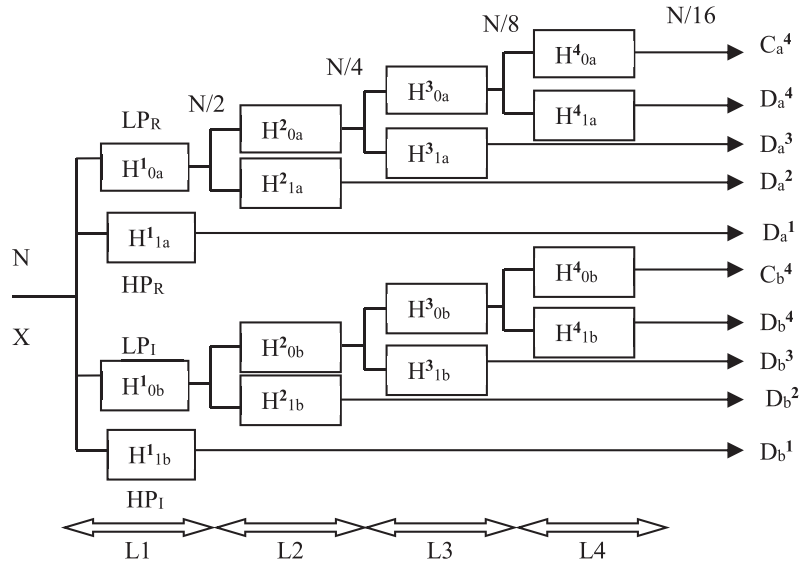


Fig. 3. DTCWT algorithm for four-level decomposition

Table 1 presents the filter coefficients used for real tree and imaginary tree of the first-level decomposition. There are 10 coefficients for each of the low-pass and high-pass filters of the real and imaginary decomposition tree structures. Table 2 presents the filter coefficients of the real tree and imaginary tree for higher levels of decomposition.

Table 1. DTCWT filter coefficients for the first stage

DTCWT filter coefficients (real)		DTCWT filter coefficients (imaginary)	
LOW PASS	HIGH PASS	LOW PASS	HIGH PASS
0	0	0.01122679215254	0
-0.08838834764832	-0.01122679215254	0.01122679215254	0
0.08838834764832	0.01122679215254	-0.08838834764832	-0.08838834764832
0.69587998903400	0.08838834764832	0.08838834764832	-0.08838834764832
0.69587998903400	0.08838834764832	0.69587998903400	0.69587998903400
0.08838834764832	-0.69587998903400	0.69587998903400	-0.69587998903400
-0.08838834764832	0.69587998903400	0.08838834764832	0.08838834764832
0.01122679215254	-0.08838834764832	-0.08838834764832	0.08838834764832
0.01122679215254	-0.08838834764832	0	0.01122679215254
0	0	0	-0.01122679215254

Table 2. DTCWT filter coefficients for a higher stage

Filter coefficients used for real tree for higher level decomposition		Filter coefficients used for imaginary tree for higher level decomposition	
LOW PASS	HIGH PASS	LOW PASS	HIGH PASS
0.03516384000000	0	0	0.03516384000000
0	0	0	0
0.08832942000000	-0.11430184000000	-0.11430184000000	0.08832942000000
0.23389032000000	0	0	0.23389032000000
0.76027237000000	0.58751830000000	0.58751830000000	0.76027237000000
0.58751830000000	-0.76027237000000	0.76027237000000	0.58751830000000
0	0.23389032000000	0.23389032000000	0
-0.11430184000000	0.08832942000000	-0.08832942000000	0.11430184000000
0	0	0	0
0	-0.03516384000000	0.03516384000000	0

3. DTCWT based PQ data compression algorithm

The DTCWT based PQ data compression algorithm is presented in Figure 4. The input raw data is pre-processed to eliminate noise. A moving average filter is used as pre-processing operation. The noise filtered PQ signal is processed by the DTCWT block to generate sub-bands. The level select input denoted by N is set to determine the number of levels required. The input N is set based on input sampling frequency. The sub-bands coefficients are processed by

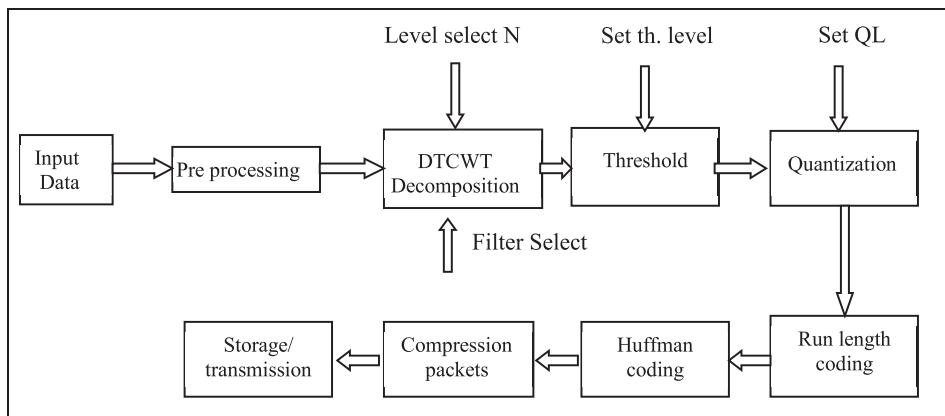


Fig. 4. Block diagram of DTCWT based PQ data compression algorithm

the thresholder and quantizer unit, by setting the threshold level and quantization level, respectively. During this process, insignificant coefficients and redundant information in the sub-bands are eliminated. The entropy encoding schemes such as Run Length Coding (RLC) and Huffman Coding, process the quantized data to achieve compression. The compressed data are grouped into packets and is prepared for storage or transmission in the smart meter sub-module and other smart grid systems.

3.1. Selection of DTCWT sub-bands

A DTCWT algorithm decomposes an input signal into multiple sub-bands, each of these sub-bands represents information in different frequency ranges varying from (sampling frequency) FS to $(FS/2)^N$. PQ disturbances such as swell, sag, harmonics and interrupts will have voltage fluctuations as well as frequency differences. Table 3 shows the frequency range in which PQ disturbances would appear.

Table 3. PQ disturbance frequency range

PQ disturbances	Frequency range
Sag	50 Hz \pm 10 Hz
Swell	50 Hz \pm 10 Hz
Harmonics	100 Hz – 500 Hz
Interrupts	> 500 Hz

The PQ undistorted signal will be a 50 Hz signal, assuming a noise reduction of 10% and the frequency of the PQ signal will be in the range of 45–55 Hz. PQ disturbances such as voltage sag and swell cause amplitude changes and hence lead to frequency fluctuations, thus the undistorted PQ signal, voltage sag and swell will also occur in the frequency band of the PQ undistorted signal. The disturbances such as harmonics and interrupts will always fall in higher frequency bands. In the novel algorithm shown in Figure 5, DTCWT decomposition is carried out to capture these signals accurately.

Eight levels of decomposition are carried out, assuming the input sampling frequency to be of 2000 Hz. The seventh- and eight-level decomposition is carried out for high-pass coefficients, as the high-pass band in level 6 holds the PQ signal of interest. The low-pass bands in level 6 are discarded. The low-pass band in level 8 is in the frequency range of 46.875 Hz to 54.0625 Hz and captures the undistorted PQ signal. The high-pass band in level 8 captures the PQ signal in frequency range of 54.0625 Hz to 62.5 Hz and hence it will contain the voltage sag and voltage swell distortions. The low-pass band in level 7 is in the frequency range of 31.25 Hz to 46.875 Hz and this band will also hold the voltage sag and swell distortions. From the 8-level decomposition the DTCWT sub-bands of importance are shown in Table 4 along with the information content. PQ events are captured in $DDC_{a/b}^8$, $DC_{a/b}^7$, $D_{a/b}^5$, $D_{a/b}^4$, $D_{a/b}^2$, $D_{a/b}^1$ sub-bands.

The events in $C_{a/b}^6$ are noise and are discarded, and the event in the $D_{a/b}^3$ band is very high harmonics, which is also discarded. The data in $DDD_{a/b}^8$ in the PQ undistorted signal is also

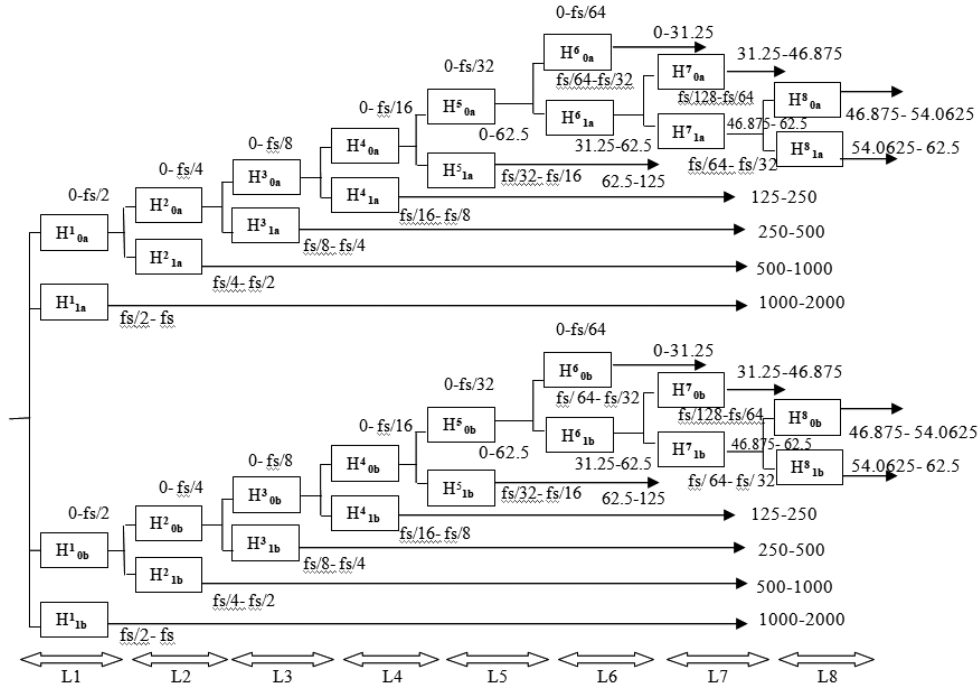


Fig. 5. DTCWT algorithms to capture PQ disturbances

Table 4. Selected DTCWT sub-bands for data compression

Band	Sub bands	Frequency Range (Hz)	PQ Signal	Threshold	Quantization
1	$DDC_{a/b}^8$	46.875–54.0625	Sag/Swell	No	Yes
2	$DDD_{a/b}^8$	54.0625–62.5	PQ undefined	Yes	Yes
3	$DC_{a/b}^7$	31.25–46.875	Sag/Swell	No	Yes
4	$C_{a/b}^6$	0–31.25	Noise	Yes	Yes
5	$D_{a/b}^5$	62.5–125	Harmonics 1	No	Yes
6	$D_{a/b}^4$	125–250	Harmonics (2–5)	No	Yes
7	$D_{a/b}^3$	250–500	Harmonics (5–10)	Yes	Yes
8	$D_{a/b}^2$	500–1 000	Interrupts	No	Yes
9	$D_{a/b}^1$	1 000–2 000	Interrupts	No	Yes

interesting. The process of quantization and thresholding is designed to retain the PQ events in bands 1, 3, 5, 6, 8, 2, 9. All other bands are discarded as the information content is very low. From the real and imaginary sub-bands only the real band low-pass coefficients are selected. As both

of them have similarly energy levels, all the eight high-pass bands are selected for encoding. The selected sub-bands at level-4 will contain PQ disturbances such as voltage sag and swell. These disturbances may also be present in the low-pass bands. The remaining three bands $\{D_{a/b}^3, D_{a/b}^2, \text{ and } D_{a/b}^1\}$ will contain all other disturbances. The $D_{a/b}^1$ sub-band will have high-frequency disturbances and will be considered as high priority.

3.2. Quantization and thresholding

The input signal of N samples after decomposition at every level of the samples is reduced by half. The intensity levels of samples at each level will also be scaled down during the decomposition process. It is found that the higher order sub-bands (high-pass bands) that hold PQ disturbances will have lower intensity levels compared with low-pass coefficients. Most of the thresholding algorithms presented in literature use a constant thresholding level across all bands of coefficients. In this algorithm, a novel thresholding algorithm is proposed to accurately capture the PQ disturbances without loss, by using a variable threshold scheme. In order to retain PQ disturbances in the high-pass bands the threshold level is set to $\{0.5, 1 \text{ and } 2\}$ for $\{D_{a/b}^1, D_{a/b}^2, \text{ and } D_{a/b}^3\}$ bands respectively. The variable thresholding algorithm is shown in Figure 6. The low-pass sub-band at the lowest level consists of real and imaginary bands, the demultiplexer unit selects either of these bands and is quantized from the first packets of the compressor. The higher order sub-bands are thresholded and quantized, so as to ensure minimum loss of data during this process. The higher order sub-bands are processed using variable thresholder and quantizer modules.

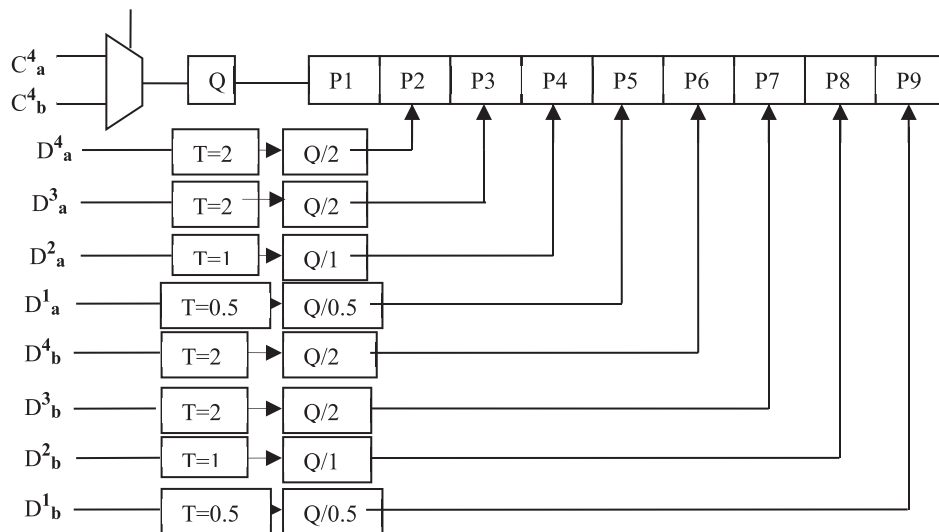


Fig. 6. Variable threshold and quantizer module

The sub-band coefficients at each level will have different intensities and hence, in order to capture the PQ disturbances without loss of data, the quantization levels are set as given in

Equations (3)–(6). By considering the maximum and minimum intensity levels at each band, the Q-levels are derived.

$$QD_{a/b}^4 = \frac{(-1 + 2^8)}{2^1} \left[\frac{D_{a/b}^4 - D_{(a/b)\max}^4}{D_{(a/b)\max}^4 - D_{(a/b)\min}^4} \right], \quad (3)$$

$$QD_{a/b}^3 = \frac{(-1 + 2^8)}{2^1} \left[\frac{D_{a/b}^3 - D_{(a/b)\max}^3}{D_{(a/b)\max}^3 - D_{(a/b)\min}^3} \right], \quad (4)$$

$$QD_{a/b}^2 = \frac{(-1 + 2^8)}{2^0} \left[\frac{D_{a/b}^2 - D_{(a/b)\max}^2}{D_{(a/b)\max}^2 - D_{(a/b)\min}^2} \right], \quad (5)$$

$$QD_{a/b}^1 = \frac{(-1 + 2^8)}{2^{-1}} \left[\frac{D_{a/b}^1 - D_{(a/b)\max}^1}{D_{(a/b)\max}^1 - D_{(a/b)\min}^1} \right]. \quad (6)$$

Due to the variable thresholding process, the detail information is not lost. Similarly, the quantizer designed is a variable quantizer. The low-pass band is quantized only to avoid loss of data. The thresholded and quantized sub-bands are combined into DTCWT packets denoted as {P1, P2, P3, P4, P5, P6, P7, P8, P9} as shown in Figure 6. The DTCWT packets are encoded using the RLC encoder and Huffman encoder. Prior to encoding of the PQ data using the RLC and Huffman encoder, the PQ metrics are detected and only these metrics are encoded. The PQ signal in general will be free from all disturbances such as sag, swell etc. the metrics of disturbances is also very significant and need to be captured. The novel approach captures these PQ metrics and compresses the metrics rather than compresses the PQ signal in total. The novel algorithm to capture PQ metrics is presented in Figure 7. The DTCWT sub-bands capture the PQ disturbances at various sub-bands depending upon the frequency of occurrence. The metrics such as time duration of disturbances, occurrence time, intensity of disturbance and frequency harmonics during disturbances are measured and are quantified with regard to the set threshold. Later they were compressed and transmitted as PQ disturbance features. Thus, the metrics provide adequate information on the PQ signal and require very less storage space.

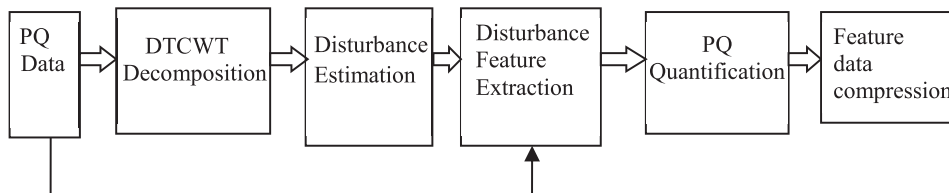


Fig. 7. Block diagram for PQ signal compression using DTCWT

Table 5 presents the energy levels of various PQ events, which are compared with the PQ signal without any disturbances (sine wave). The energy level of the sine wave is around 8 units,

all other disturbances do not fall in this range and hence there is a clear demarcation between PQ events that assist in determining the event and its metrics.

Table 5. Energy levels of various PQ events

DTCWT	Sine	Swell	Sag	Harmonics	Harmonics with swell	Harmonics with sag	Interrupts
Energy level	8.01	43.925	28.374	40.66864	30.13071	44.87097	6.8300

Figure 8 illustrates the novel algorithm for PQ metric estimation. The DTCWT decomposition gives rise to 10 sub-bands. Each of the sub-bands is processed and is verified for PQ disturbances. If the PQ event is swell and sag, the time duration of the swell and sag is determined by computing the maximum gradient of each sub-band. The time duration determined is superimposed on the PQ signal and the fluctuations in voltage is computed in reference to average PQ signal intensity. Similarly, if the Q event is harmonics or interruptions, THD is computed and the total duration of these events occurred is also determined. If the PQ events are below the set PQ standards, they are discarded. Only the signals, which are very significant are encoded into packets by the algorithm shown in Figure 8. To verify their functionality, the input signals representing power line distortions are mathematically modelled. The controlled parameters are used in the mathematical model for generation of various distortions. The input signal is generated for certain time duration, it is divided into multiple frames of size 2048 samples. Each frame of data is processed using DTCWT and 10 sub-bands are computed along with the energy levels, which have unique values for various distortions as shown in Figure 9. Based on the unique values of

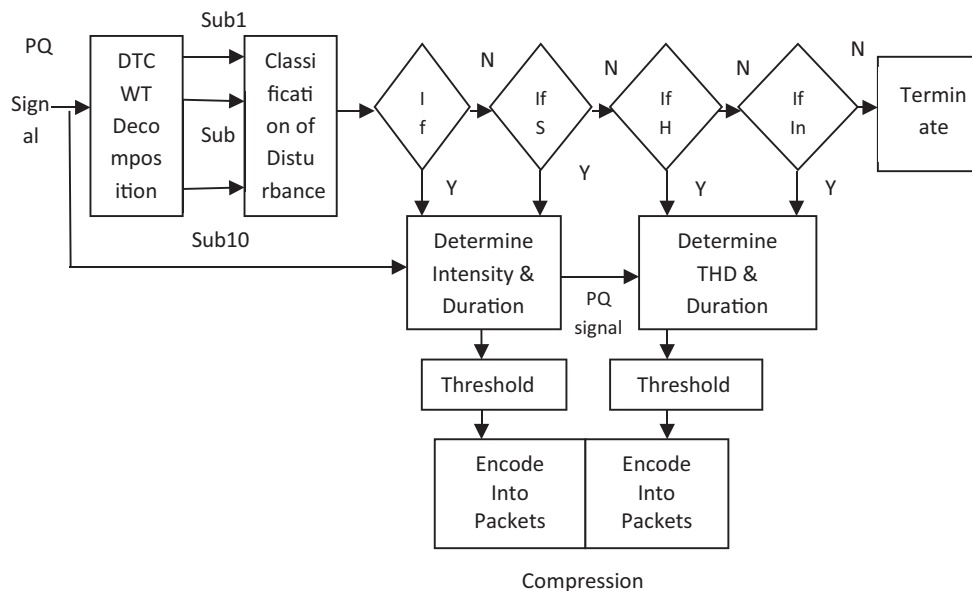


Fig. 8. Block diagram for classification of PQ disturbances

energy levels, PQ classification is performed. PQ distortion is identified and based on the classification algorithm along with the time-frequency information obtained it is used to characterize the input.

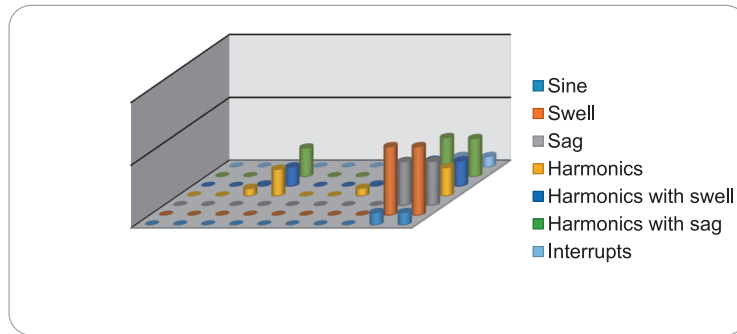


Fig. 9. Energy levels of 10 sub-bands of various PQ events

4. Software modeling and implementation

A PQ analyser EN50160 module is connected to capture real time PQ parameters along with a net meter (a sub-set of smart grid environment), which is connected between the source and load.

Figure 10 shows the general block diagram of a grid connected PV inverter system, having solar panels that provide most of their power needed during the daytime, while still being connected to the local electrical grid network during the night-time. The excess electricity generated during the daytime is not wasted but it is fed back into the power grid. The PQ analyser is connected externally to an inverter side to measure the variation of RMS voltage and other parameters. The PQ data recorded from 10.11.16 to 12.11.16 are mentioned, just to represent the real time data extracted by the PQ analyser, which has been connected externally as shown in Figure 11.

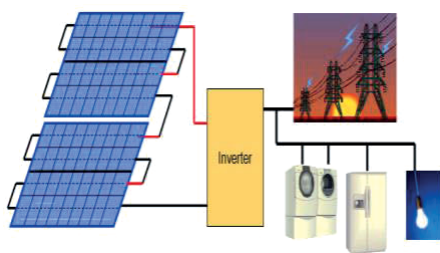


Fig. 10. General diagram of solar grid connected inverter



Fig. 11. PQ analyzer connected to extract the data

The data login module is connected to one phase of the grid and the PQ data is recorded continuously for four days. The recorder or the data login module captures RMS values, calculated

in each half-period (10 ms at 50 Hz, 8.3 ms at 60 Hz), which are out of the thresholds set upon configuration by 1% to 30% of a set reference value with a 1% step. To validate the proposed algorithm, RMS values of raw voltage data are considered from the PQ data recorder instrument.

Figure 12 shows the RMS voltages of the PQ data recorded from 10.11.16 to 12.11.16 and only the average RMS voltages of 4300 data samples are plotted. For PQ signal analysis, the average RMS values are used to generate an actual PQ signal of 50 Hz sine wave. The disturbances are recorded and stored in a storage unit in the PQ instrument. The memory card reader is removed and the recorded PQ data is accessed in offline mode in Matlab environment for analysis. Figure 13 shows the experimental setup for validation of the proposed algorithm. The PQ data captured online is stored in a computer in Excel format and the data is read in the Matlab environment for off line analysis. The developed software module loads the power signal data and computes the DTCWT coefficients. The DTCWT coefficients after quantization and thresholding are encoded using RLC and Huffman Encoders. The compressed data stored in the Matlab environment is processed to estimate the memory storage requirement. The compressed data is decompressed using the inverse DTCWT and inverse encoding process to obtain the reconstructed PQ data. The error in reconstruction processes is evaluated by computing MSE, PSNR and the maximum error.

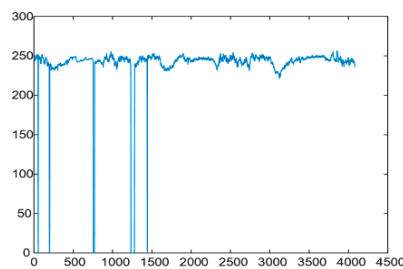


Fig. 12. Recorded voltage data in pixels

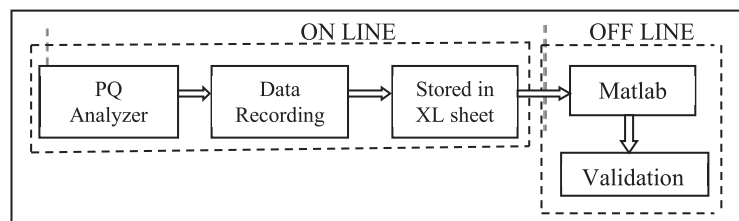


Fig. 13. Experimental setup of PQ data analysis

The length of the input data is determined to identify the number of bits, similarly the compressed data is evaluated to identify the number of bits required after compression. The compression ratio is determined by evaluating the input sequence length and the encoded sequence length. The performance parameters such as MSE, maximum error and PSNR are computed by evaluating the input data and the decompressed output data. The proposed algorithm is modelled in Matlab and the performance metrics for data compression is computed to evaluate the advantages of the DTCWT based compression algorithm as shown in Figure 14.

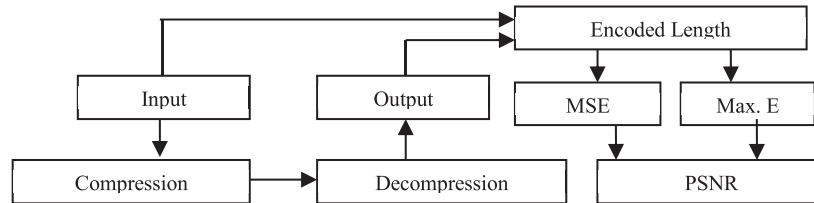


Fig. 14. Performance evaluation setup

5. Results and discussion

The developed MATLAB code for compression of a PQ signal is executed by considering the recorded PQ signal. The distorted PQ signal is presented in Figure 15. The DTCWT algorithm, which is designed to compute eight levels of decomposition processes, the PQ signal and the results are presented in Figure 16. Figure 17 presents the DTCWT results of a low-pass real sub-band that comprises of 17 000 samples. The interrupts in the PQ data are seen as voltage dips.

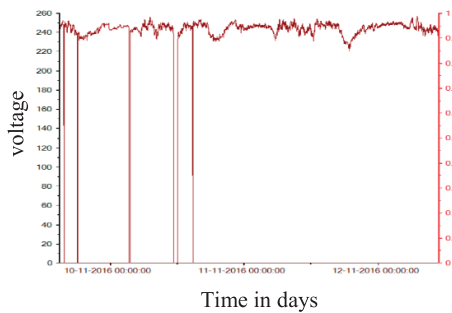


Fig. 15. PQ analyzer recorded voltage data for 3 days

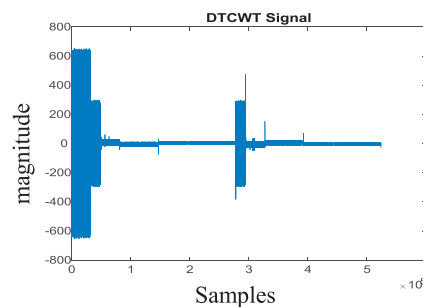


Fig. 16. DTCWT sub-bands

Figure 18 presents the results of the DTCWT sub-bands after thresholding and quantization. The quantization process reduces the number of bits required to represent DTCWT samples, thus constituting compression. The proposed quantization and thresholding logic ensures that the data loss does not exceed more than 2 dB.

The quantized DTCWT sub-bands are entropy encoded using RLC and Huffman coding. The compressed PQ data is reconstructed by performing an inverse process. The reconstructed PQ signal is compared with the input data and performance metrics such as a PSNR and compression ratio are computed. Table 6 presents comparison results of PQ data samples compressed using the DTCWT with optimum thresholding and quantization, the DTCWT and DWT based algorithm for five sets of data recorded at different time intervals. The proposed algorithm for PQ compression considers only the significant sub-bands and the corresponding threshold and quantization levels are set to achieve better compression and reconstruction. The proposed Modified Dual Tree Complex Wavelet Transform algorithm is denoted in Table 7 as “MDTCWT”. The PQ

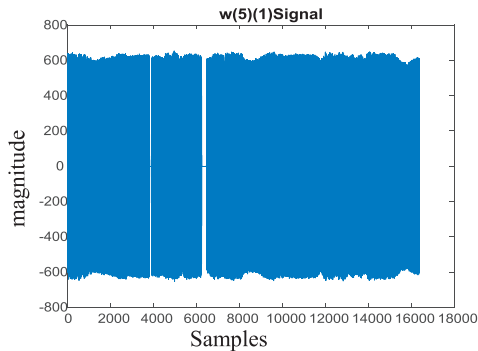


Fig. 17. DTCWT low pass real sub-band

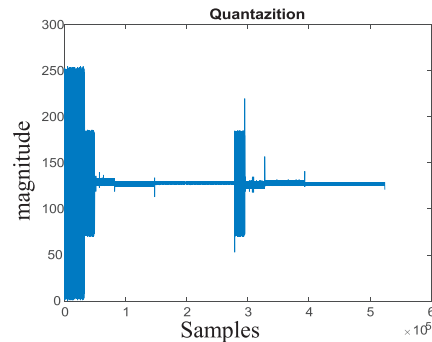


Fig. 18. DTCWT sub-bands after quantization and thresholding

data samples recorded for certain duration have an input sequence length of 2 975 778 samples (each of 8-bit) and are compressed to 954 253 samples. The compression ratio is determined to be 67.9327 with a maximum error of 5.8139, MSE of 3.7343 and PSNR of 42.4732. The compression ratio achieved using the DWT based algorithm is found to be superior to the DTCWT based algorithm, however the PSNR obtained for the proposed algorithm is better than the DWT based algorithm. The number of sub-bands in the DTCWT is twice as high as it is in the DWT and hence it restricts the compression ratio. The redundancy in the real and imaginary DTCWT sub-bands is identified and eliminated to improve the compression ratio without affecting the PSNR. The results of the MDTCWT algorithm in terms of a compression ratio and PSNR is found to be better than with the use of the DWT and DTCWT based algorithms for PQ compression. With selection of bands, selection of threshold levels and the quantization algorithm, the proposed PSNR of the MDTCWT is improved by a factor of 3% as compared with the DTCWT based PQ compression algorithm. Similarly, the compression ratio is also improved by a factor of 16%.

Table 6. Comparison of DWT and DTCWT results

Real time data samples	PSNR			Compression ratio		
	DWT	DTCWT	MDTCWT	DWT	DTCWT	MDTCWT
sample1	42.2111	42.4732	88.4021	82.7240	67.9327	81.2391
sample2	38.5949	40.5795	70.3797	99.2550	98.2096	99.7821
sample3	34.2399	40.8719	60.2698	98.5620	96.9110	99.1711
sample4	36.1726	40.1784	71.8160	98.5095	96.7771	99.4112
sample5	36.1757	39.4565	70.3452	98.5598	96.9174	99.0145

Eight-level DTCWT generates 18 sub-bands, of which 9 are real and 9 of them are imaginary. The shift invariant property of the DTCWT is demonstrated by considering both of these bands.

For compression of data only the real or the imaginary bands could be considered. In order to improve compression ratio beyond 50%, the phase information needs to be computed and significance of data loss needs to be analysed by considering the real and imaginary information.

Table 7. Comparison of Compression performance of different methods

PQ data	Energy threshold and adaptive arithmetic encoding [5]		Using integrated spline wavelet and S-transform [9]		Proposed MDTCWT method	
	CR	NMSE	CR	NMSE	CR	NMSE
Real time voltage data	7.09%	1.42×10^{-3}	5.0633	2.5088×10^{-4}	32.0673	1.64×10^{-4}

Table 7 gives the comparison of the proposed method with the reference papers on energy threshold and adaptive arithmetic encoding [5] as well as using integrated spine wavelet and S-transform [9]. With respect to a compression ratio and normalized mean square error, this proposed DTCWT produces a higher compression ratio and obtains a smaller mean square error.

6. Conclusion

Smart grid technology will provide better power supply services and eventually revolutionize the power generation and distribution management services. A smart meter, which is the sub-component of a smart grid, will need to be able to provide services for data logging, storage and transmission. The data compression algorithm proposed in this work achieves a compression ratio of greater than 90% with minimum loss of data measured in terms of a PSNR achieving more than 42 dB. DTCWT sub-bands that support shift invariant property and directionality produce more than 28 sub-bands and hence have redundancy of data. The selective thresholding technique and quantization modules ensure that the information content or PQ signal features are selected from the DTCWT bands and are encoded to achieve required compression ratios. With selective logic, desired compression can be achieved for PQ signals and hence supports real time application requirements of smart meters, which have an additional feature of variable data compression schemes that is compatible to the needs of available transmission bandwidth or data rate requirements.

References

- [1] <http://ibm.com/software/data/industry/energy.html>, accessed May 2012.
- [2] <http://netl.doe.gov/moderngrid>, accessed January 2007.
- [3] Norman C.F., Chan Y.C., Lau W-H., *Real-Time Power-Quality Monitoring with Hybrid Sinusoidal and Lifting Wavelet Compression Algorithm*, IEEE Transactions on power Delivery, vol. 27, iss. 4, pp. 1718–1726 (2012).
- [4] Bingham R.P., Kreiss D., Santoso S., *Advances in data reduction techniques for power quality Instrumentation*, Proceeding of 3rd European Power Quality Conference, Bremen, Germany, pp. 47–55 (1995).

- [5] Wang J., Wang C., *Compression of Power Quality Disturbance Data Based on Energy Threshold and Adaptive Arithmetic Encoding*, TENCON-2005, IEEE region10 Conference, Melbourne, Qld, Australia, pp. 1–4 (2005).
- [6] Zhang D., Bi Y., Zhao J., *A new data compression algorithm for power quality online monitoring*, Proceeding of International Conference on Sustainable Power Generation and Supply, China, pp. 1–4 (2009).
- [7] Ning J., Wang J., Gao W., Liu C., *A wavelet-based data compression technique for smart grid*, IEEE Transactions on Smart Grid, vol. 2, no. 1, pp. 212–218 (2011).
- [8] Parseh R., Acevedo S.S., Kansanen K., Molinas M., Ramstad T.A., *Real-time compression of Measurements in distribution grids*, Proceeding of 3rd International conference, Smart Grid Communication, Tainan City, Taiwan, pp. 223–228 (2012).
- [9] Dash P.K., Panigrahi B.K., Sahoo D.K., Panda G., *Power Quality Disturbance Data Compression, Detection, and Classification Using Integrated Spline Wavelet and S-Transform*, IEEE Transactions on Power Delivery, vol. 18, no. 2, pp. 595–600 (2003).
- [10] Mohammadzadeh S., Seifossadat S., Ahmadzadeh M., *Power Quality Disturbance Data Compression Using Wavelets Transform*, International Conference on Computer, Systems and Electronics Engineering, South Africa, Johannesburg, pp. 78–82 (2014).
- [11] Zhao Hongtu, Xi Dongmei, *Compression and Realization of Power Quality Disturbance Data Based on Wavelet Analysis*, International Conference on Uncertainty Reasoning and Knowledge Engineering, Bali, Indonesia, pp. 217–219 (2011).
- [12] Yi Zhong, Cheng Chen, Hang Su, *Measurement and Analysis for Power Quality Using Compressed Sensing*, Journal of Applied Science and Engineering, vol. 17, no. 3, pp. 305–318 (2014).
- [13] Santoso S., Powers E.J., Grady W.M., *Power quality disturbance data compression using wavelet transform methods*, IEEE Transactions on Power Delivery, vol. 12, no. 3, pp. 1250–1257 (1997).
- [14] Albu M.M., Neurohr R., Apetrei D., Silvas I., *Monitoring voltage and frequency in smart distribution grids. A case study on data compression and accessibility*, Published in Power and Energy Society General Meeting, 2010 IEEE, Providence, RI, USA, pp. 1–6 (2010).
- [15] Zhang Li, Ma Shiqiang, *An Improved Method Based on Wavelet for Power Quality Compression*, 2016 IEEE 11th Conference on Industrial Electronics and Applications (ICIEA), Hefei, China, pp. 1750–1753 (2016).